Biochimica et Biophysica Acta 1824 (2012) 647–655

Contents lists available at SciVerse ScienceDirect

Biochimica et Biophysica Acta

journal homepage: www.elsevier.com/locate/bbapap

Kinetic characterisation of *o*-aminophenols and aromatic *o*-diamines as suicide substrates of tyrosinase

Jose Luis Muñoz-Muñoz [a], Francisco Garcia-Molina [a], Jose Berna [b], Pedro Antonio Garcia-Ruiz [c], Ramon Varon [d], Jose Tudela [a], Jose N. Rodriguez-Lopez [a], Francisco Garcia-Canovas [a,*]

[a] GENZ: Grupo de Investigación Enzimología, Departamento de Bioquímica y Biología Molecular-A, Facultad de Biología, Universidad de Murcia, E-30100, Espinardo, Murcia, Spain
[b] Departamento de Química Orgánica, Facultad de Química, Universidad de Murcia, E-30100, Espinardo, Murcia, Spain
[c] QCPAI: Grupo de Química de Carbohidratos, Polímeros y Aditivos Industriales, Departamento de Química Orgánica, Facultad de Química, Universidad de Murcia, E-30100, Espinardo, Murcia, Spain
[d] Departamento de Química-Física, Escuela de Ingenieros Industriales de Albacete, Universidad de Castilla la Mancha, Avda. España s/n. Campus Universitario, E-02071, Albacete, Spain

ARTICLE INFO

Article history:
Received 9 November 2011
Received in revised form 31 January 2012
Accepted 1 February 2012
Available online 10 February 2012

Keywords:
Tyrosinase
Aromatic *o*-diamine
o-Aminophenol
Suicide inactivation
o-Diphenol

ABSTRACT

We study the suicide inactivation of tyrosinase acting on *o*-aminophenols and aromatic *o*-diamines and compare the results with those obtained for the corresponding *o*-diphenols. The catalytic constants follow the order aromatic *o*-diamines < *o*-aminophenols < *o*-diphenols, which agrees with the view that the transfer of the proton to the peroxide group of the oxy-tyrosinase form is the slowest step in the catalytic cycle. As regards the apparent inactivation constant, it remains within the same order of magnitude, although slightly lower in the case of the aromatic *o*-diamines and *o*-aminophenols than *o*-diphenols: *o*-diamines < *o*-aminophenols < *o*-diphenols. The efficiency of the second nucleophilic attack of substrate on CuA seems to be the determining factor in the bifurcation of the inactivation and catalytic pathways. This attack is more efficient in *o*-diamines (where it attacks a nitrogen atom) than in *o*-aminophenols and *o*-diphenols (where it attacks an oxygen atom), favouring the catalytic pathway and slowing down the inactivation pathway. The inactivation step is the slowest of the whole process. The values of *r*, the number of turnovers that 1 mol of enzyme carries out before being inactivated, follows the order aromatic *o*-diamines < *o*-aminophenols < *o*-diphenols. As regards the Michaelis constants, that of the *o*-diamines is slightly lower than that of the *o*-diphenols, while that of the *o*-aminophenols is slightly greater than that observed for the *o*-diphenols. As a consequence of the above, the inactivation efficiency, λ_{max}/K_m^S, follows this order: *o*-diphenols > *o*-aminophenols > aromatic *o*-diamines.

1. Introduction

Tyrosinase is a cuproprotein that catalyses the hydroxylation of monophenols to *o*-diphenols (monophenolase activity) and the oxidation of the latter to *o*-quinones (diphenolase activity), using molecular oxygen [1–3].

Tyrosinase suffers inactivation when it reacts with its *o*-diphenolic and triphenolic substrates [4–11]. The catalytic process is related with the nucleophilic power of the oxygen atom of the hydroxyl group bound to the carbon atom in *para* position with respect to the R group (C-4). However, the inactivation process has no such direct relation, and substrates with low chemical shift (δ) values in C-4 have a high catalytic constant but low inactivation constant. The relation between these constants is given by the parameter *r*, the number of turnovers that 1 mol of enzyme carries out before being inactivated.

The crystallisation of tyrosinase from different sources, *Streptomyces castaneoglobisporus* [12], *Bacillus megaterium* [13,14] and *Agaricus bisporus* [15], has increased our knowledge of the structure of the enzyme. In addition, it has been described that mushroom tyrosinase has an active centre close to the surface [15], which would explain the low substrate specificity shown by this enzyme [16–20].

Kinetic studies in the transition phase and the steady state have shown that the *o*-diphenols bind to the form met-tyrosinase (E_m) more rapidly than to the form oxy-tyrosinase (E_{ox}) [21]. Furthermore, studies on the isotopic effect in the presence of deuterated water have suggested that the transfer of a proton from the hydroxyl group of C-4 to the peroxide group of E_{ox} is the rate-limiting step in both diphenolase and monophenolase activities [22,23].

Experiments using aromatic monoamines, aromatic *o*-diamines and *o*-aminophenols as substrates [20,24–27] point to the low values of the catalytic constant of these processes, lending support to the suggestion that the transfer of the critical proton to the oxy-tyrosinase form is the limiting step in the catalytic cycle [20,24,25]. In an earlier publication, we studied the catalytic action of tyrosinase

* Corresponding author. Tel.: +34 868 884764; fax: +34 868 883963.
E-mail address: canovasf@um.es (F. Garcia-Canovas).

1570-9639/$ – see front matter © 2012 Elsevier B.V. All rights reserved.
doi:10.1016/j.bbapap.2012.02.001

on aromatic monoamines, aromatic *o*-diamines and *o*-aminophenols, which were found to be substrates of the enzyme [20]. When the reactions above were followed at long measurement times, the suicide inactivation of tyrosinase was evident [5–7]. The wide variety of aromatic *o*-diamines and *o*-aminophenols that are available commercially has enabled us to look more deeply at this suicide inactivation process by studying their corresponding structure/reactivity relationships.

2. Material and methods

2.1. Materials

Mushroom tyrosinase or polyphenol oxidase (TYR, *o*-diphenol: O_2 oxidoreductase, EC 1.14.18.1) (8300 units/mg) and L-ascorbic acid (AH_2) were supplied by Sigma (Madrid, Spain). The enzyme was purified as previously described in Ref. [21]. Protein concentration was determined by the Lowry method [28]. All the substrates used in this work were purchased from Sigma (Madrid, Spain) (Table 1SM). All other chemicals were of analytical grade. Stock solutions of the *o*-diphenolic substrates, aromatic *o*-diamines and *o*-aminophenols were prepared in 0.15 mM phosphoric acid to prevent autooxidation. Milli-Q system (Millipore Corp.) ultrapure water was used throughout.

2.2. Methods

2.2.1. Spectrophotometric assays

These assays were carried out with a Perkin-Elmer Lambda-35 (Perkin-Elmer, Massachusetts, USA) spectrophotometer, on line interfaced to a PC-computer, where the kinetic data were recorded, stored and later analysed. The products of the enzyme reaction (*o*-quinoneimine or *o*-diimine) are unstable and evolve towards other products [24,29]. For this reason, the reaction was followed by measuring the disappearance of AH_2 at the wavelength and molar absorptivity coefficient specified for each substrate (Table 2SM). This coupled reagent reduces *o*-quinone to *o*-diphenol, *o*-quinoneimine to *o*-aminophenol and *o*-diimines to *o*-diamines, respectively [20,30,31]. The substrates used in this method were 2-aminophenol, 3-amino-4-hydroxybenzoic acid, 4-amino-3-hydroxybenzoic acid, 3-amino-L-tyrosine, 1,2-diaminobenzene, 3,4-diaminotoluene, 4-methoxy-1,2-phenylenediamine and 2,3-diaminobenzoic acid.

2.2.2. Oxymetric assays

When the substrate and ascorbic acid spectra overlapped, oxymetric assays were carried out [32]. Measurements of dissolved oxygen concentration were made with a Hansatech (Kings Lynn, Cambs, U.K.) oxygraph unit controlled by a PC. The oxygraph used a Clark-type silver/platinum electrode with a 12.5 μm Teflon membrane. The sample was continuously stirred during the experiments and its temperature was maintained at 25 °C. The zero oxygen level for calibration and the experiments was obtained by bubbling oxygen-free nitrogen through the sample for at least 10 min. The substrates 3-amino-4-hydroxytoluene, 4-amino-3-hydroxytoluene, 2-amino-3-hydroxybenzoic acid, 3-amino-2-hydroxybenzoic acid, 3,4-diaminobenzoic acid, 2,3-dihydroxybenzoic acid, 4-fluor-1,2-phenylenediamine, 4-chloro-1,2-phenylenediamine and 4-bromo-1,2-phenylenediamine were studied by means of this method.

The effect of various reagents, whose concentrations are given in detail in the corresponding figures of Section 3, was studied. In all the assays, the following reagents were maintained constant: 0.26 mM O_2 (saturating), 30 mM phosphate buffer pH 7.0 and the concentration of AH_2 that is indicated in the corresponding figure legend.

2.2.3. Data analysis

The experimental data of time-based assays for the disappearance of AH_2 follow Eq. (1):

$$[AH_2] = [AH_2]_f + [AH_2]_\infty e^{-\lambda^S_{E_{ox}} t} \quad (1)$$

where $[AH_2]_f$ is the AH_2-value at $t \to \infty$, $[AH_2]_\infty = [Q]_\infty$ is the AH_2 consumed at the end of the reaction and $\lambda^S_{E_{ox}}$ is the apparent constant of suicide inactivation of tyrosinase in the presence of the corresponding

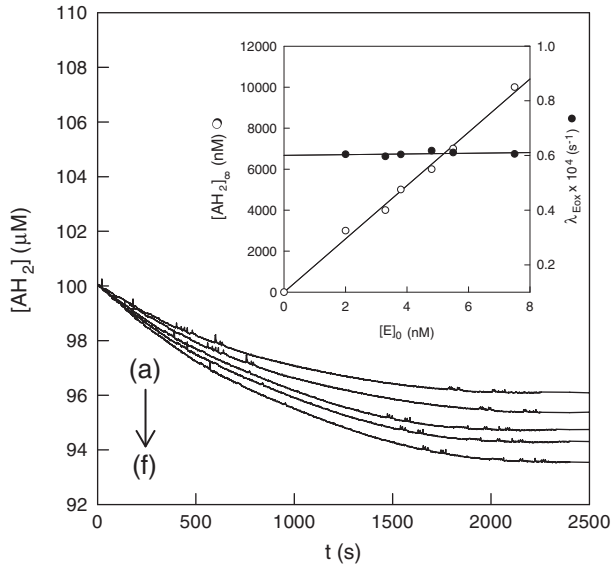

Fig. 1. Corrected recordings of the disappearance of AH_2 in the suicide inactivation of tyrosinase by the oxidation of 3,4-diaminotoluene for different enzyme concentrations. The experimental conditions were 30 mM sodium phosphate buffer (pH 7.0), 0.1 mM AH_2, 0.26 mM O_2, wavelength = 265 nm, the initial substrate concentration, $[S]_0 = 0.1$ mM, and the initial enzyme concentration, $[E]_0$, (nM): (a) 2, (b) 3.3, (c) 3.8, (d) 4.8, (e) 5.5 and (f) 7.5. Inset. Representation of the values of $[AH_2]_\infty$ (○) and $\lambda^S_{E_{ox}}$ (•) *vs.* enzyme concentration.

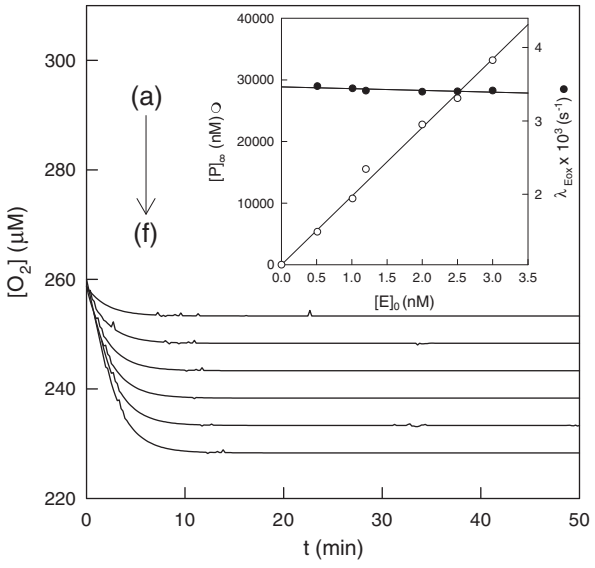

Fig. 2. Corrected recordings of the disappearance of oxygen in the suicide inactivation of tyrosinase by the oxidation of 3-amino-4-hydroxytoluene for different enzyme concentrations. The experimental conditions were 30 mM sodium phosphate buffer (pH 7.0), 0.15 mM AH_2, 0.26 mM O_2, $[S]_0 = 5$ mM and $[E]_0$ (nM): (a) 0.5, (b) 1, (c) 1.2, (d) 2, (e) 2.5 and (f) 3. Inset. Representation of the values of $[O_2]_\infty$ (○) and $\lambda^S_{E_{ox}}$ (•) *vs.* enzyme concentration.

Table 1
Kinetic constants characterising the suicide inactivation of tyrosinase acting on aromatic *o*-diamines.

Aromatic *o*-diamine	$\lambda_{E_{ox}(max)}{}^{S}$ x 10^3 (s^{-1})	*r*	k^S_{cat} (s^{-1})	K^S_m (mM)	k_6 (M^{-1} s^{-1})	δ_1 (ppm)	δ_2 (ppm)	δ_3 (ppm)	δ_4 (ppm)	$\Sigma\delta$ (ppm)
4-Fluor-1,2-phenylenediamine	3.87 ± 0.32	31 ± 3	0.12 ± 0.01	0.24 ± 0.03	500 ± 58	128.9	134.9	–	–	263.8
4-Bromo-1,2-phenylenediamine	3.75 ± 0.35	16 ± 2	0.06 ± 0.01	0.73 ± 0.10	82 ± 11	132.3	135.5	–	–	267.8
4-Chloro-1,2-phenylenediamine	2.57 ± 0.18	35 ± 3	0.09 ± 0.01	0.52 ± 0.07	173 ± 19	131.4	134.7	–	–	266.1
4-Methoxy-1,2-phenylenediamine	1.77 ± 0.12	852 ± 89	1.48 ± 0.15	0.38 ± 0.06	3894 ± 416	125.6	134.3	–	–	259.9
1,2-Diaminobenzene	1.47 ± 0.09	360 ± 31	0.51 ± 0.06	0.44 ± 0.04	1159 ± 132	133.3	133.3	–	–	266.6
3,4-Diaminotoluene	0.85 ± 0.09	599 ± 51	0.54 ± 0.05	0.07 ± 0.01	7714 ± 892	–	–	133.2	130.3	263.5
3,4-Diaminobenzoic acid	0.81 ± 0.07	98 ± 9	0.07 ± 0.01	0.13 ± 0.02	538 ± 58	–	–	127.2	132.4	259.6
2,3-Diaminobenzoic acid	0.57 ± 0.05	88 ± 7	0.04 ± 0.01	0.30 ± 0.04	133 ± 11	–	134.3	135.9	–	270.2

Table 2
Kinetic constants characterising the suicide inactivation of tyrosinase acting on *o*-aminophenols.

o-Aminophenol	$\lambda_{E_{ox}(max)}{}^{S} \times 10^3$ (s^{-1})	*r*	k^S_{cat} (s^{-1})	K^S_m (mM)	k_6 (M^{-1} s^{-1})	δ_1 (ppm)	δ_2 (ppm)	δ_3 (ppm)	δ_4 (ppm)	$\Sigma\delta$ (ppm)
2-Aminophenol	7.90 ± 0.09	7666 ± 815	58.12 ± 2.84	0.82 ± 0.09	70,878 ± 7502	143.9	133.9	–	–	277.8
3-Amino-4-hydroxytoluene	5.34 ± 0.39	5503 ± 502	25.02 ± 1.58	2.77 ± 0.59	9032 ± 918	–	–	133.8	140.9	274.7
4-Amino-3-hydroxytoluene	4.43 ± 0.41	5884 ± 510	21.72 ± 2.13	2.33 ± 0.41	9322 ± 950	–	–	143.8	130.9	274.7
3-Amino-L-tyrosine	2.01 ± 0.17	701 ± 65	1.21 ± 0.15	0.96 ± 0.20	1260 ± 121	–	–	133.8	141.1	274.9
4-Amino-3-hydroxybenzoic acid	0.62 ± 0.04	810 ± 76	0.48 ± 0.01	0.14 ± 0.01	3429 ± 315	–	–	144.1	139.1	283.2
3-Amino-4-hydroxybenzoic acid	0.37 ± 0.02	1230 ± 101	0.43 ± 0.01	0.13 ± 0.01	3308 ± 295	–	–	132.8	147.7	280.5
3-Amino-2-hydroxybenzoic acid	0.93 ± 0.07	140 ± 8	0.15 ± 0.01	0.39 ± 0.05	384 ± 39	–	150.6	134.7	–	285.3
2-Amino-3-hydroxybenzoic acid	1.38 ± 0.11	94 ± 7	0.15 ± 0.01	2.20 ± 0.24	68 ± 7	–	137.4	145.4	–	282.8

o-diphenol, *o*-aminophenol or aromatic *o*-diamine. These parameters can be obtained by non-linear regression [33]. There is always a slow spontaneous oxidation of *o*-diphenol, *o*-aminophenol, aromatic *o*-diamine and AH_2 (result not shown), which should be computer corrected in further [AH_2] *vs.* time plots (in general this treatment is applied to all the kinetic recordings). Fig. 1 shows the recordings for the oxidation of 3,4-diaminotoluene. Kinetic analysis of these recordings according to Eq. (1) provides the values of $[AH_2]_\infty$ and $\lambda_{E_{ox}}{}^{S}$. The inset of Fig. 1 reveals the dependence of these parameters on the enzyme concentration.

When the disappearance of oxygen is measured, the experimental data of time-based assays for the disappearance follow Eq. (2):

$$[O_2] = [O_2]_f + [O_2]_\infty e^{-\lambda^S_{Eox} t} \quad (2)$$

where $[O_2]_f$ is the O_2-value at $t \to \infty$, $[O_2]_\infty$ is the O_2 consumed at the end of the reaction and $\lambda^S_{E_{ox}}$ is the apparent constant of suicide inactivation of tyrosinase in the presence of the corresponding substrate. These parameters can be obtained by non-linear regression [33]. Note that $[O_2]_\infty$ becomes $[Q]_\infty/2$, reflecting the stoichiometry of the reaction. Fig. 2 depicts the recordings for the disappearance of oxygen during the oxidation of 3-amino-4-hydroxytoluene. Fitting these data to Eq. (2) gives the values of $[O_2]_\infty$ and $\lambda^S_{E_{ox}}$. The dependence of these parameters on the enzyme concentration can be seen from Fig. 2 inset.

2.2.4. Determination of ^{13}C NMR chemical shifts

The carbon chemical shifts given in Tables 1–3 were obtained from the corresponding ^{13}C NMR spectra, which were recorded at 298 K on a Bruker Avance 400 MHz instrument employing buffered solutions (at pH = 7.0) of pure samples in D_2O. For those compounds that were insoluble in this medium (4-fluor-1,2-phenylenediamine, 4-chloro-1,2-phenylenediamine, 4-bromo-1,2-phenylenediamine, 4-methoxy-1,2-phenylenediamine, *o*-phenylenediamine, 3,4-diaminotoluene, 2-aminophenol, 3-amino-4-hydroxytoluene, 4-amino-3-hydroxytoluene and 3-amino-L-tyrosine), the respective chemical shifts were estimated with the ChemNMR module included in the ChemDraw v8.0, a CambridgeSoft Desktop Software and corrected with the chemical shifts of the corresponding head compound (*o*-phenylenediamine, 2-aminophenol, *o*-catechol).

3. Results and discussion

The suicide inactivation kinetic of tyrosinase acting on aromatic *o*-diamines and *o*-aminophenols was studied. From this study, the kinetic parameters that characterise the suicide inactivation process were obtained: the maximum apparent suicide constant ($\lambda_{E_{ox}(max)}{}^{S}$), the catalytic constant (k^S_{cat}) and the parameter *r* which represents the number of turnovers that 1 mol of enzyme makes before it is inactivated.

3.1. Oxidation of aromatic *o*-diamines

Scheme 1 represents a proposed mechanism to explain the catalytic oxidation of aromatic *o*-diamines, which takes into account (*i*) the suicide inactivation [6] and (*ii*) the studies carried out with 3,6-difluorocatechol, in which the existence of two kinetically significant pK's is evident [34]. Kinetic studies measuring the initial velocity

Table 3
Kinetic constants characterising the suicide inactivation of tyrosinase acting on *o*-diphenols.

o-Diphenol	$\lambda_{E_{ox}(max)}{}^{S} \times 10^3$ (s^{-1})	*r*	k^S_{cat} (s^{-1})	K^S_m (mM)	$k_6 \times 10^{-3}$ (M^{-1} s^{-1})	δ_1 (ppm)	δ_2 (ppm)	δ_3 (ppm)	δ_4 (ppm)	$\Sigma\delta$ (ppm)
Catechol	8.92 ± 0.27	99,994 ± 1604	874.1 ± 30.2	0.16 ± 0.01	5463.13 ± 568.21	146.59	146.59	–	–	293.18
4-Chlorocatechol	8.54 ± 0.25	99,356 ± 1377	859.2 ± 28.3	0.60 ± 0.03	1432.00 ± 148.02	145.04	147.35	–	–	292.39
4-Methylcatechol	8.21 ± 0.25	98,366 ± 1377	842.1 ± 26.1	0.10 ± 0.01	8421.00 ± 853.34	144.06	146.43	–	–	290.49
L-Dopa	2.21 ± 0.01	46,133 ± 2306	102.6 ± 19.2	0.55 ± 0.08	186.55 ± 19.36	–	–	146.92	146.06	292.98
2,3-Dihydroxybenzoic acid	0.96 ± 0.08	386 ± 40	0.39 ± 0.05	1.09 ± 0.14	0.36 ± 0.05	–	149.01	143.89	–	292.90
3,4-Dihydroxybenzoic acid	0.85 ± 0.03	10,186 ± 224	8.11 ± 0.30	0.07 ± 0.01	115.86 ± 13.62	–	–	146.04	150.00	296.04

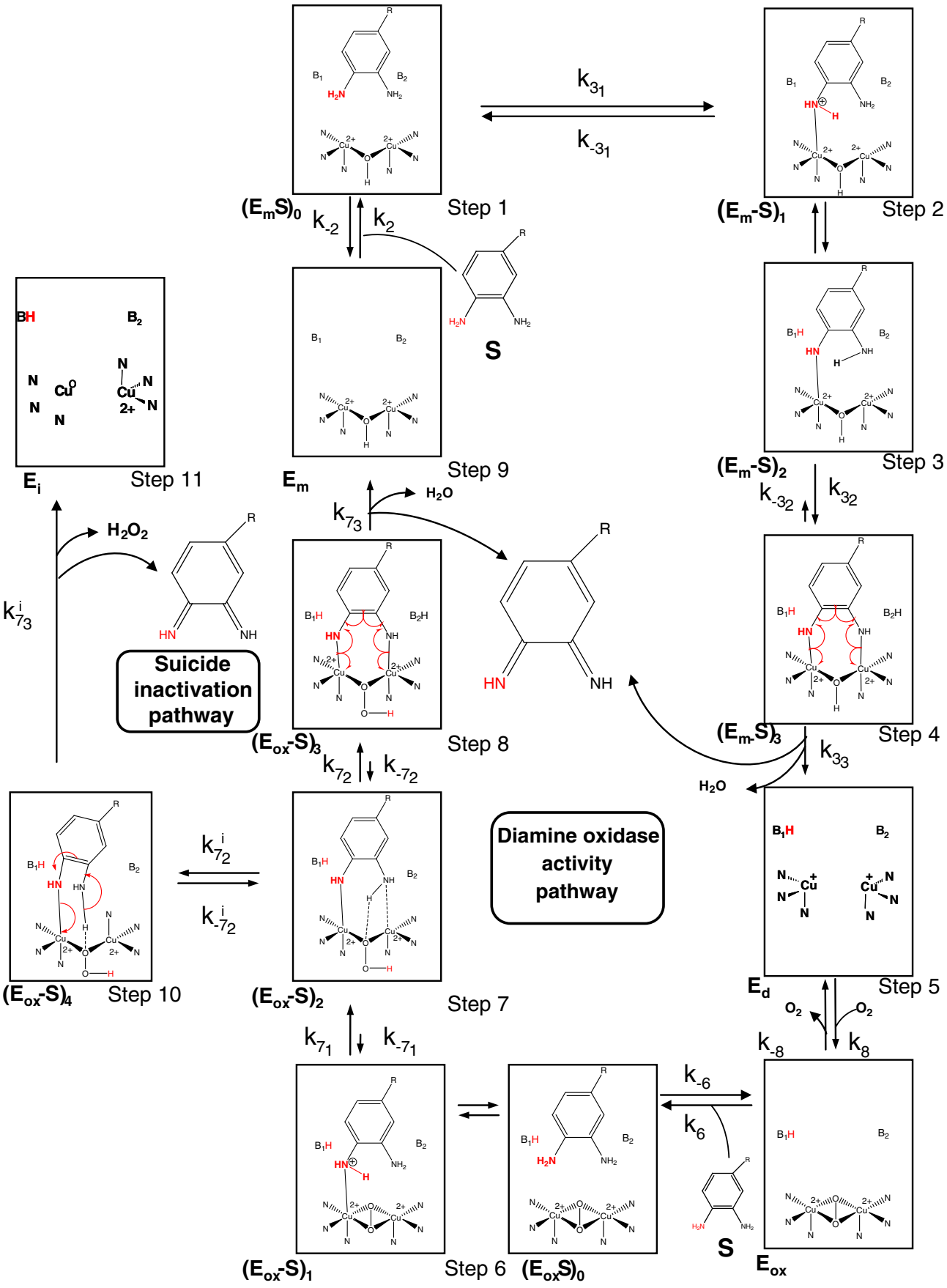
$(E_mS)_0$
Step 1
$(E_m\text{-}S)_1$
Step 2
$(E_m\text{-}S)_2$
Step 3
$(E_m\text{-}S)_3$
Step 4
E_d
Step 5
E_{ox}
$(E_{ox}S)_0$
Step 6
$(E_{ox}\text{-}S)_1$
Step 7
$(E_{ox}\text{-}S)_2$
Step 8
E_m
Step 9
$(E_{ox}\text{-}S)_3$
Step 10
$(E_{ox}\text{-}S)_4$
E_i
Step 11
S
k_{31}
k_{-31}
k_{-2}
k_2
k_{32}
k_{-32}
k_{33}
k_{73}
k^i_{73}
k_{72}
k_{-72}
k^i_{72}
k^i_{-72}
k_{71}
k_{-71}
k_{-6}
k_6
k_{-8}
k_8
H_2O
H_2O_2
O_2
Suicide inactivation pathway
Diamine oxidase activity pathway

gave the catalytic constant (k^S_{cat}) and the Michaelis constant (K^S_m) (Table 1) [20]. Fig. 3 shows the recordings of the disappearance of AH_2 during the oxidation of 3,4-diaminotoluene, at long measuring times. Fig. 3 inset shows the values $\lambda^S_{E_{ox}}$ [obtained by means of Eq. (1)] for different concentrations of 3,4-diaminotoluene. Therefore, the hyperbolic behaviour observed in this representation allows us the calculation of $\lambda^S_{E_{ox}(max)}$ and K^S_m for this compound, according to Eq. (3) (Table 1) [6].

$$\lambda^S_{E_{ox}} = \frac{\lambda^S_{E_{ox}(max)}[S]_0}{K^S_m + [S]_0} \quad (3)$$

In the case of the oxidation of aromatic *o*-diamines, the velocity of catalysis reflected in the value of the catalytic constant (k^S_{cat}) is very low compared with those of the corresponding *o*-diphenols. This is because Step 7 in Scheme 1 is much slower due to the proton transfer from an amino group is less unlikely (compared when this transfer is produced from a hydroxyl group). This slowing down of the catalytic pathway has no effect on the suicide inactivation pathway because this process is limiting (Tables 1–3). From the values of $\lambda^S_{E_{ox}(max)}$ obtained for the aromatic *o*-diamines (Table 1) and bearing in mind the ^{13}C NMR values of these molecules (Table 1), it is deduced that (a) the substitution of oxygen by nitrogen slows down both the catalysis and suicide inactivation; (b) the first nucleophilic attack on CuB in Step 2 and Step 6 is always carried out by the nitrogen bound to the carbon atom with the lowest chemical shift (δ) in an attack that is facilitated by base 1 (B_1); (c) the second nitrogen atom can carry out a nucleophilic attack on the CuA, transferring the proton to the second base (B_2) or to the peroxide group of the oxy-tyrosinase form; (d) the lower the value of δ of the carbon atom that carries the NH_2 group responsible for the second attack on the CuA, the more nucleophilic the nature of the nitrogen, and so the catalytic pathway is preferred to the inactivation pathway and the apparent inactivation constant is lower; and (e) the sum of the chemical shifts of the carbon atoms that carry the diamine groups, will be responsible for the values of k^S_{cat}; hence, the lower the sum of the δ values, the greater the k^S_{cat}. Based on these predictions, the order of the aromatic *o*-diamines is given in Table 1.

The compounds 3,4-diaminobenzoic acid and 2,3-diaminobenzoic acid deserve additional comment. Taking into account its δ_3 and δ_4 values, 3,4-diaminobenzoic acid (Table 1) should have a low $\lambda^S_{E_{ox}(max)}$ and one of the highest k^S_{cat}. In the case of 2,3-diaminobenzoic acid, as the attack on the CuB is carried out by the C-2 group, a possible steric hindrance means that the behaviour of this compound could well differ from the predicted behaviour (see Table 1). The carboxylic group of 3,4-diaminobenzoic acid might inhibit tyrosinase, diminishing k^S_{cat}, $\lambda^S_{E_{ox}(max)}$ and K^S_m; in this case, 3,4-diaminobenzoic would be acting as a stoichiometric inhibitor with the substrate [35,36].

When the data shown in Table 1 for the aromatic *o*-diamines are compared with those obtained for *o*-diphenols (Table 3) k^S_{cat} can be seen to be smaller by three orders of magnitude, but the apparent inactivation constant ($\lambda^S_{E_{ox}(max)}$) remains in the same range, so that the value of *r* is much lower (by approximately three orders of magnitude) in the aromatic *o*-diamines (Tables 1 and 3).

The values of the Michaelis constants for the aromatic *o*-diamines are low (Table 1) and of a similar order of magnitude to those of the *o*-diphenols (Table 3), while the Michaelis constants of the *o*-aminophenols (Table 2) are greater, since

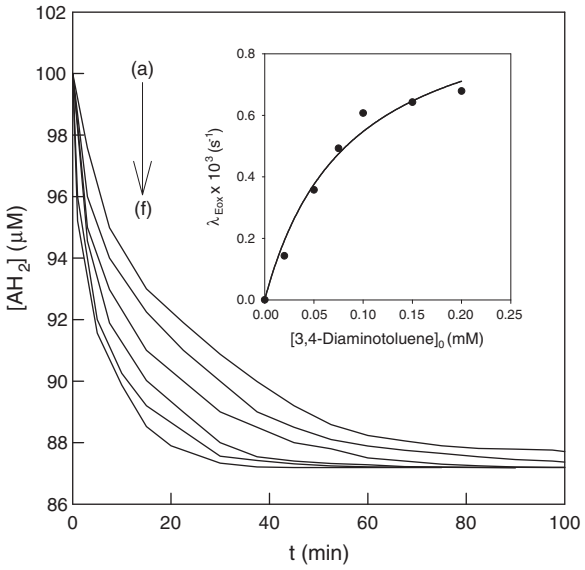

Fig. 3. Corrected recordings of the disappearance of AH_2 in the suicide inactivation of tyrosinase by the oxidation of different 3,4-diaminotoluene concentrations. The experimental conditions were 30 mM sodium phosphate buffer (pH 7.0), 0.26 mM O_2, wavelength = 265 nm and the initial concentrations of AH_2 and tyrosinase were 0.1 mM and 30 nM, respectively. The substrate concentrations were (mM) (a) 0.02, (b) 0.05, (c) 0.075, (d) 0.1, (e) 0.15 and (f) 0.2. Inset. Values of $\lambda^S_{E_{ox}}$ for different 3,4-diaminotoluene concentrations.

$$K^S_m = \frac{k^S_{cat}}{k_6} \quad (4)$$

The aromatic *o*-diamines have low k^S_{cat}, K^S_m and k_6 values (Table 1). We have postulated that it can be due that these compounds have an electron-rich ring and then repulsive π–π interactions with, probably, a histidine residue of the active site could established [37]. *o*-diphenols (Table 3) have high k^S_{cat} and k_6 values [21], and the ring of the substrate is less electron-rich and so there should be weaker repulsion at the active site. In the case of *o*-aminophenols (Table 2), the catalytic constant values, k^S_{cat}, are higher than those corresponding to the aromatic *o*-diamines and so K^S_m is slightly higher (see Eq. (4)). Thus, the k_6 values are lower in the case of aromatic *o*-diamines than in the case of *o*-diphenols (Tables 2 and 3).

3.2. Oxidation of o-aminophenols

The mechanism proposed to explain the catalytic oxidation and the suicide inactivation of *o*-aminophenols is described in Scheme 2. Fig. 4 shows the recordings obtained when varying the concentration of substrate in the oxidation of 3-amino-4-hydroxytoluene. Fig. 4 inset depicts the hyperbolic dependence of $\lambda^S_{E_{ox}}$ *vs.* $[S]_0$, while analysis using Eq. (3) permits us to obtain $\lambda^S_{E_{ox}(max)}$ and K^S_m. When the oxidation of the *o*-aminophenols is studied, the catalytic constants are greater than those obtained for the corresponding aromatic *o*-diamines (Tables 1 and 2) and lower than those of the *o*-diphenols (Table 3). The slowest step in the catalysis should be Step 7—the transfer of the proton to the peroxide group in oxy-tyrosinase. The

Scheme 1. Structural mechanism proposed to explain the catalytic and suicide inactivation pathways of tyrosinase in its action on aromatic *o*-diamines. E_m, met-tyrosinase; $(E_mS)_0$, met-tyrosinase/aromatic *o*-diamine complex; $(E_m–S)_1$, met-tyrosinase/aromatic *o*-diamine complex axially bound to a CuB atom with the base (B_1) forming a hydrogen bridge; $(E_m–S)_2$, met-tyrosinase/aromatic *o*-diamine complex axially bound to a CuB atom with protonated base (B_1H); $(E_m–S)_3$, met-tyrosinase/aromatic *o*-diamine complex axially bound to the two Cu atoms; E_d, deoxy-tyrosinase; E_{ox}, oxy-tyrosinase; $(E_{ox}S)_0$, oxy-tyrosinase/aromatic *o*-diamine complex; $(E_{ox}–S)_1$, oxy-tyrosinase/aromatic *o*-diamine complex axially bound to a CuB atom; $(E_{ox}–S)_2$, oxy-tyrosinase/aromatic *o*-diamine complex axially bound to the CuB atom and with the proton transferred to the peroxide group; $(E_{ox}–S)_3$, oxy-tyrosinase/aromatic *o*-diamine complex axially bound to the two Cu atoms with one proton transferred to the peroxide group and the other proton transferred to the base B_2 (B_2H); $(E_{ox}–S)_4$, oxy-tyrosinase/aromatic *o*-diamine complex axially bound to the CuB atom and with two protons transferred to the peroxide group; E_i, enzyme inactive.

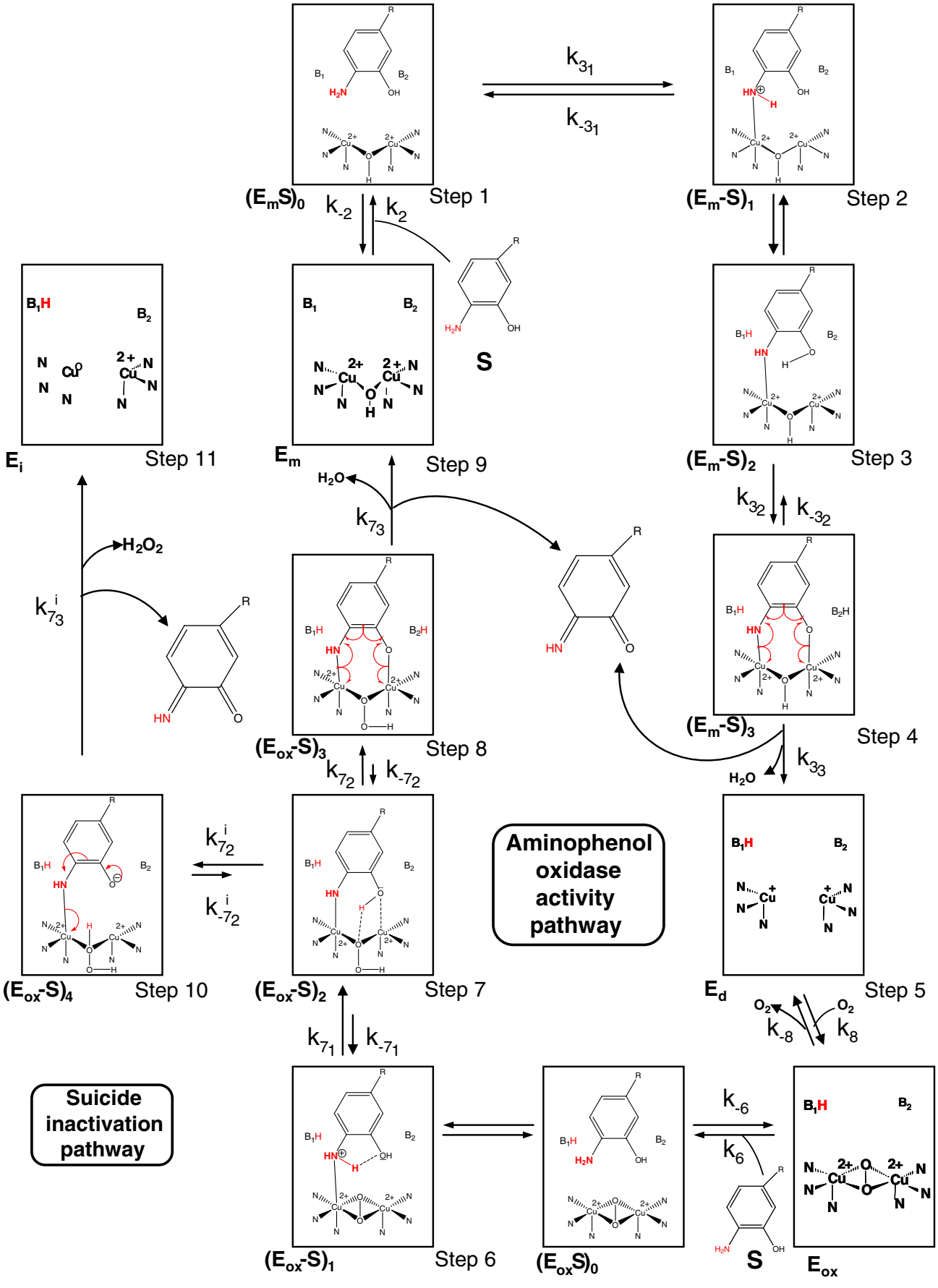
$(E_mS)_0$
Step 1
k_{31}
k_{-31}
$(E_m\text{-}S)_1$
Step 2
k_{-2}
k_2
S
E_i
Step 11
E_m
Step 9
$(E_m\text{-}S)_2$
Step 3
H_2O
k_{73}
k_{32}
k_{-32}
H_2O_2
k_{73}^i
$(E_{ox}\text{-}S)_3$
Step 8
$(E_m\text{-}S)_3$
Step 4
k_{72}
k_{-72}
H_2O
k_{33}
k_{72}^i
k_{-72}^i
Aminophenol oxidase activity pathway
$(E_{ox}\text{-}S)_4$
Step 10
$(E_{ox}\text{-}S)_2$
Step 7
E_d
Step 5
O_2
k_{-8}
O_2
k_8
k_{71}
k_{-71}
Suicide inactivation pathway
$(E_{ox}\text{-}S)_1$
Step 6
$(E_{ox}S)_0$
k_{-6}
k_6
S
E_{ox}

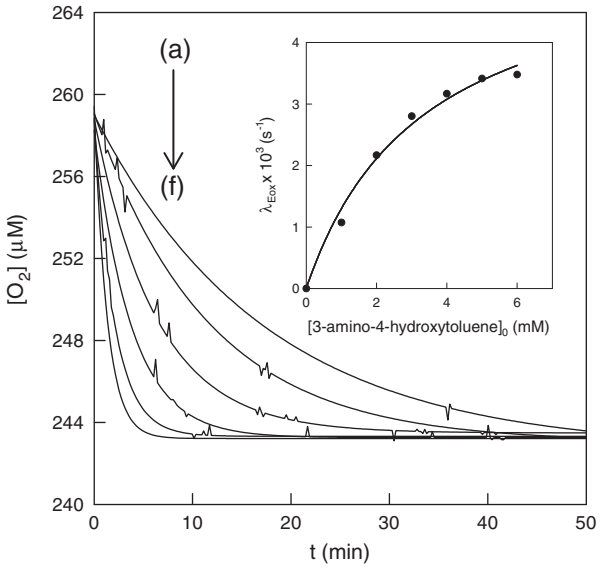

Fig. 4. Corrected recordings of the disappearance of oxygen in the suicide inactivation of tyrosinase by the oxidation of different 3-amino-4-hydroxytoluene concentrations. The experimental conditions were 30 mM sodium phosphate buffer (pH 7.0), 0.26 mM O_2 and the initial concentrations of AH_2 and tyrosinase were 0.15 mM and 2 nM, respectively. The substrate concentrations were (mM) (a) 1, (b) 2, (c) 3, (d) 4, (e) 5 and (f) 6. Inset. Values of $\lambda^S_{E_{ox}}$ for different 3-amino-4-hydroxytoluene concentrations.

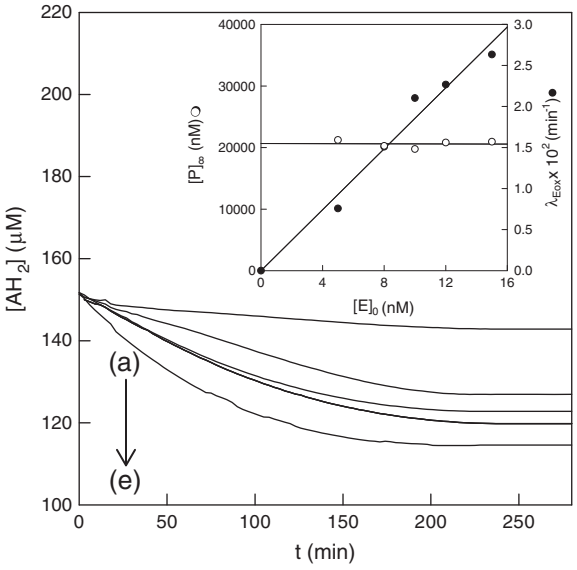

Fig. 5. Corrected recordings of the disappearance of AH_2 in the suicide inactivation of tyrosinase by the oxidation of 3-amino-4-hydroxybenzoic acid for different enzyme concentrations. The experimental conditions were 30 mM sodium phosphate buffer (pH 7.0), 0.15 mM AH_2, 0.26 mM O_2, wavelength = 280 nm, $[S]_0 = 0.37$ mM and $[E]_0$ (nM): (a) 5, (b) 8, (c) 10, (d) 12 and (e) 15. Inset. Representation of the values of $[AH_2]_\infty$ (○) and $\lambda^S_{E_{ox}}$ (•) *vs.* enzyme concentration.

speed of the suicide inactivation will depend on the efficiency of the nucleophilic attack of the oxygen atom of the hydroxyl group. In principle, the substrate attack will always occur through the amino group on the CuB and then of the oxygen atom of the hydroxyl group on CuA. Depending on the δ value of the carbon atom carrying the hydroxyl group, the catalytic or inactivation pathway will be favoured. When the δ value is low, the nucleophilic attack of the oxygen atom of the hydroxyl group on the copper atom (CuA) would be favoured and the proton transferred to base B_2 thereby favouring the catalytic pathway over the inactivation pathway. In this way, the value of $\lambda^S_{E_{ox}(max)}$ would be lower than in the case of *o*-diphenols. The results depicted in Table 2 agree with this reasoning. The catalytic constants are lower than for the *o*-diphenols, but, in this case, only by one order of magnitude (Tables 2 and 3). The apparent inactivation constants remain within the same order of magnitude as those corresponding to *o*-diphenols but are lower (Tables 2 and 3), which agrees with the behaviour of the aromatic *o*-diamines, suggesting that the slowest step of the whole process (inactivation pathway) is the transfer of a proton from the amine group (aromatic *o*-diamines) or the hydroxyl group (*o*-aminophenols and *o*-diphenols) to the peroxide group in the form E_{ox} (Tables 1–3).

Table 2 shows the compounds ordered by the decreasing value of $\lambda^S_{E_{ox}(max)}$, where, in addition, it is possible to distinguish between the compounds bearing -OH (2-aminophenol) or $-CH_3$ (3-amino-4-hydroxytoluene and 4-amino-3-hydroxytoluene) in C-1, and the group bearing $-CH_2-CHNH_2-COOH$ (3-amino-L-tyrosine). In this way, it is possible to distinguish the derivates of benzoic acid, which, as mentioned above, may inhibit the enzyme through carboxylic group. Such compounds would act as stoichiometric inhibitors, and so k^S_{cat}, K^S_m and $\lambda^S_{E_{ox}(max)}$ would decay. Figs. 5 and 6 show the recordings for the oxidation of 3-amino-4-hydroxybenzoic acid obtained byz varying the concentrations of enzyme and substrate, respectively. Fig. 5 inset and Fig. 6 inset show the dependence of $[AH_2]_\infty$ and $\lambda^S_{E_{ox}}$ on these concentrations. As can be seen, the concentration of $[AH_2]_\infty$ is

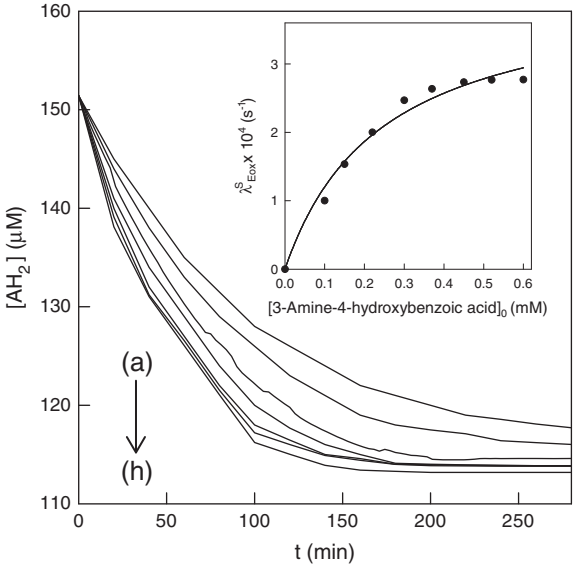

Fig. 6. Corrected recordings of the disappearance of AH_2 in the suicide inactivation of tyrosinase by the oxidation of different 3-amino-4-hydroxybenzoic acid concentrations. The experimental conditions were 30 mM sodium phosphate buffer (pH 7.0), 0.26 mM O_2, wavelength = 280 nm and the initial concentrations of AH_2 and tyrosinase were 0.15 mM and 15 nM, respectively. The substrate concentrations were (mM) (a) 0.1, (b) 0.15, (c) 0.22, (d) 0.3, (e) 0.37, (f) 0.45, (g) 0.52 and (h) 0.6. Inset. Values of $\lambda^S_{E_{ox}}$ for different 3-amino-4-hydroxybenzoic acid concentrations.

Scheme 2. Structural mechanism proposed to explain the catalytic and suicide inactivation pathways of tyrosinase in its action on *o*-aminophenols. E_m, met-tyrosinase; $(E_mS)_0$, met-tyrosinase/*o*-aminophenol complex; $(E_m–S)_1$, met-tyrosinase/*o*-aminophenol complex axially bound to a CuB atom; $(E_m–S)_2$, met-tyrosinase/*o*-aminophenol complex axially bound to a CuB atom with the proton transferred to the base B_1 (B_1H); $(E_m–S)_3$, met-tyrosinase/*o*-aminophenol complex axially bound to the two Cu atoms with the proton of the OH group transferred to the base B_2 (B_2H); E_d, deoxy-tyrosinase; E_{ox}, oxy-tyrosinase; $(E_{ox}S)_0$, oxy-tyrosinase/*o*-aminophenol complex; $(E_{ox}–S)_1$, oxy-tyrosinase/*o*-aminophenol complex axially bound to a CuB atom; $(E_{ox}–S)_2$, oxy-tyrosinase/*o*-aminophenol complex axially bound to the CuB atom and with the proton transferred to the peroxide group; $(E_{ox}–S)_3$, oxy-tyrosinase/*o*-aminophenol complex axially bound to the two Cu atoms with one proton transferred to the peroxide group and the other proton transferred to the base B_2 (B_2H); $(E_{ox}–S)_4$, oxy-tyrosinase/*o*-aminophenol complex axially bound to the CuB atom with two protons transferred to the peroxide group; E_i, inactive enzyme.

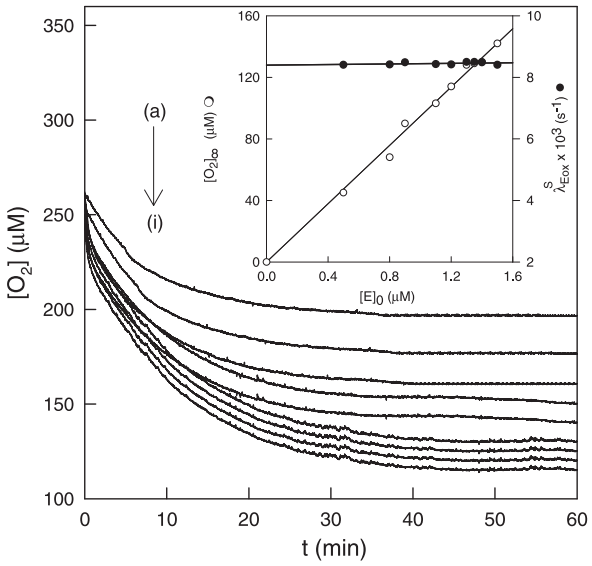

Fig. 7. Corrected recordings of the disappearance of oxygen in the suicide inactivation of tyrosinase by the oxidation of 2-amino-3-hydroxybenzoic acid for different enzyme concentrations. The experimental conditions were 30 mM sodium phosphate buffer (pH 7.0), 0.15 mM AH_2, 0.26 mM O_2, $[S]_0 = 3$ mM and $[E]_0$ (nM): (a) 0.5, (b) 0.8, (c) 0.9, (d) 1.1, (e) 1.2, (f) 1.3, (g) 1.35, (h) 1.4 and (i) 1.5. Inset. Representation of the values of $[O_2]_\infty$ (○) and $\lambda_{E_{ox}}{}^S$ (•) *vs.* enzyme concentration.

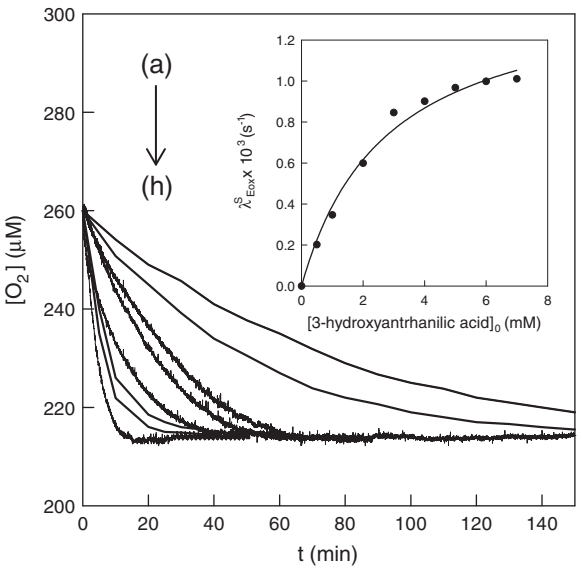

Fig. 8. Corrected recordings of the disappearance of oxygen in the suicide inactivation of tyrosinase by the oxidation of different 2-amino-3-hydroxybenzoic acid concentrations. The experimental conditions were 30 mM sodium phosphate buffer (pH 7.0), 0.26 mM O_2 and the initial concentrations of AH_2 and tyrosinase were 0.15 mM and 0.5 μM, respectively. The substrate concentrations were (mM) (a) 0.5, (b) 1, (c) 2, (d) 3, (e) 4, (f) 5, (g) 6 and (h) 7. Inset. Values of $\lambda_{E_{ox}}{}^S$ for different 2-amino-3-hydroxybenzoic acid concentrations.

directly proportional to the enzyme concentration, while $\lambda^S_{E_{ox}}$ is independent (Fig. 5 inset). However, $\lambda^S_{E_{ox}}$ shows a hyperbolic behaviour *vs.* the substrate concentration, while $[AH_2]_\infty$ is independent (Fig. 6 inset). By means of Eq. (3) it is possible to obtain $\lambda^S_{E_{ox}(max)}$ and K^S_m (Table 2). Figs. 7 and 8 depict the recordings of the disappearance of oxygen during the oxidation of 2-amino-3-hydroxybenzoic acid by tyrosinase, varying the enzyme and substrate concentrations, respectively. Fig. 7 inset depicts the values of $[O_2]_\infty$ and $\lambda^S_{E_{ox}}$ *vs.* enzyme concentration. Fig. 8 inset represents $\lambda^S_{E_{ox}}$ vs. the substrate concentration. From Eq. (3), it is possible to obtain $\lambda^S_{E_{ox}(max)}$ and K^S_m (Table 2). The results are similar to those obtained in the insets of Figs. 5 inset and 6.

Table 2 shows that the compound 2-aminophenol has the highest k^S_{cat} and, as the δ value of the carbon atom carrying the hydroxyl group is high, its $\lambda^S_{E_{ox}(max)}$ is also high and the *r* is the highest in Table 2. Its K^S_m is higher than that of catechol, possibly because the binding constant to the enzyme (k_6) is hindered by the repulsion involved in the π–π interactions (Table 2). As can be seen, the derivates of toluene show similar values of k^S_{cat} and $\lambda^S_{E_{ox}(max)}$ and, therefore, of *r*. Note that the Michaelis constants are one order of magnitude higher than that corresponding to 4-methylcatechol even though the k^S_{cat} is one order of magnitude less, probably because the lower binding constant (k_6) resulting from the greater electron density of the aromatic ring would hinder the binding (see Table 2). In the case of 3-amino-L-tyrosine, the nitrogen in C-3 would be responsible for the binding in CuB; the δ_4 value is very high and so the catalytic constant falls to 1.41 s^{-1}; furthermore, the first attack on CuB occurs through the amino group bound to C-3, and the Michaelis constant increases with respect to L-dopa, pointing to steric hindrances, as has been described previously for the compounds 2-amino-3-hydroxybenzenesulphonamide and 3-amino-2-hydroxybenzenesulphonamide [38].

In the case of the benzoic acid derivates, as in the case of aromatic *o*-diamines, the carboxylic group may react with the copper atoms, inhibiting the enzyme and resulting in an apparent diminution of k^S_{cat}, $\lambda^S_{E_{ox}(max)}$ and K^S_m [35,36]. Note the low values of these parameters in Table 2 and how the carbon atoms that support the NH_2 group have a lower δ value. In the same way, the withdrawing effect of the carboxylic group is stronger if the substituent in C-4 is a hydroxyl group. This is confirmed by comparing the 3-amino-4-hydroxybenzoic acid and 3-hydroxy-4-aminobenzoic acid, which have similar k^S_{cat}, $\lambda^S_{Eox}(max)$, K^S_m and *r* values. In the case of ortho derivates, the results are practically identical to those obtained for the dihydroxylated derivates (Tables 2 and 3) except that the K^S_m is higher in 2-amino-3-hydroxybenzoic acid (3-hydroxyanthranilic acid). The attack carried out by C-2 (CuB) points to the steric hindrance involved in the increase in K^S_m [38].

The results described above highlight the importance of proton transfer from the aromatic *o*-diamines and *o*-aminophenols to the peroxide group in the oxy-tyrosinase. During the catalysis, two transfers may occur to the oxy-tyrosinase, one to base B_2 and the other to the peroxide group in what is probably the limiting step (Step 7 in Schemes 1 and 2). The transfer of two protons probably occurs during suicide inactivation as well, but, in this case, both are transferred to the peroxide group of the oxy-tyrosinase. The first nucleophilic attack of the oxygen atom from the hydroxyl group involving the transfer of the first proton to the peroxide group is the limiting step of the catalysis, while the deprotonation involving no nucleophilic attack of the oxygen atom of the second hydroxyl group is the limiting step in the inactivation (Step 10 en Schemes 1 and 2). As regards Schemes 1 and 2, the first proton to the peroxide group corresponds to Step 7 in both cases (limiting step of the catalysis). The catalytic pathway continues in both Schemes with Step 8, in which the proton is transferred to base B_2. The inactivation pathway in both Schemes continues with Step 10, both for aromatic *o*-diamines (Scheme 1) and *o*-aminophenols (Scheme 2). This step would be limiting for the suicide inactivation.

Supplementary materials related to this article can be found online at doi:10.1016/j.bbapap.2012.02.001.

Acknowledgements

This paper was partially supported by grants from Ministerio de Educación y Ciencia (Madrid, Spain) Project BIO2009-12956, Fundación Séneca (CARM, Murcia, Spain) Projects 08856/PI/08 and 08595/PI/08, and Consejería de Educación (CARM, Murcia, Spain) BIO-BMC 06/01-0004. JLMM and FGM hold two fellowships from Fundación Caja Murcia

(Murcia, Spain). J.B. thanks the MICINN for a Ramon y Cajal Fellowship, co-financed by the European Social Fund.

References

[1] E.I. Solomon, U.M. Sundaram, T.E. Machonkin, Multicopper oxidases and oxygenases, Chem. Rev. 96 (1996) 2563–2606.
[2] M. Rolff, J. Schottenheim, H. Decker, F. Tuczek, Copper-O_2 reactivity of tyrosinase models towards external monophenolic substrates: molecular mechanism and comparison with the enzyme, Chem. Soc. Rev. 40 (2011) 4077–4098.
[3] L. Casella, E. Monzani, M. Gulloti, D. Cavagino, G. Cerina, L. Santagostini, R. Ugo, Functional modelling of tyrosinase. Mechanism of phenol ortho hydroxylation by dinuclear copper complexes, Inorg. Chem. 35 (1996) 7516–7625.
[4] J. Escribano, J. Tudela, F. Garcia-Carmona, F. Garcia-Canovas, A kinetic study of the suicide inactivation of an enzyme measured through coupling reactions, Biochem. J. 262 (1989) 597–603.
[5] J.L. Munoz-Munoz, F. Garcia-Molina, R. Varon, P.A. Garcia-Ruiz, J. Tudela, F. Garcia-Canovas, J.N. Rodriguez-Lopez, Suicide inactivation of the diphenolase and monophenolase activities of tyrosinase, IUBMB Life 62 (2010) 539–547.
[6] J.L. Muñoz-Muñoz, F. Garcia-Molina, P.A. Garcia-Ruiz, M. Molina-Alarcon, J. Tudela, F. Garcia-Canovas, J.N. Rodriguez-Lopez, Phenolic substrates and suicide inactivation of tyrosinase: kinetics and mechanism, Biochem. J. 416 (2008) 413–440.
[7] J.L. Muñoz-Muñoz, J.R. Acosta-Motos, F. Garcia-Molina, R. Varon, P.A. Garcia-Ruíz, J. Tudela, F. Garcia-Cánovas, J.N. Rodríguez-López, Tyrosinase inactivation in its action on L-dopa, Biochim. Biophys. Acta 1804 (2010) 1467–1475.
[8] T.S. Chang, Two potent suicide substrates of mushroom tyrosinase, J. Agric. Food Chem. 55 (2007) 2010–2015.
[9] T.S. Chang, M.Y. Lin, H.J. Lin, Indentifying 8-hydroxynaringenin as a suicide substrate of mushroom tyrosinase, J. Cosmet. Sci. 61 (2010) 205–210.
[10] S.S.-K. Tai, C.-G. Lin, M.-H. Wu, T.S. Chang, Evaluation of depigmenting activity by 8-hydroxydaidzein in mouse B16 melanoma cells and human volunteers, Int. J. Mol. Sci. 10 (2009) 4257–4266.
[11] E.J. Land, C.A. Ramsden, P.A. Riley, The mechanism of suicide-inactivation of tyrosinase: a substrate structure investigation, Tohoku J. Exp. Med. 212 (2007) 341–348.
[12] Y. Matoba, T. Kumagai, A. Yamamoto, H. Yoshitsu, M. Sugiyama, Crystallographic evidence that the dinuclear copper center of tyrosinase is flexible during catalysis, J. Biol. Chem. 281 (2006) 8981–8990.
[13] M. Sendovski, M. Kanteev, V. Shuster Ben-Yosef, N. Adir, A. Fishman, Crystallization and preliminary X-ray crystallographic analysis of a bacterial tyrosinase from *Bacillus megaterium*, Acta Crystallogr. Sect. F Struct. Biol. Cryst. Commun. 66 (2010) 1101–1103.
[14] M. Sendovski, M. Kanteev, V. Shuster Ben-Yosef, N. Adir, A. Fishman, First structures of an active bacterial tyrosinase reveal copper plasticity, J. Mol. Biol. 405 (2011) 227–237.
[15] W.T. Ismaya, H.J. Rozeboom, A. Weijn, J.J. Mes, F. Fusetti, H.J. Wichers, W.B. Dijkstra, Crystal structure of *Agaricus bisporus* mushroom tyrosinase: identity of the tetramer subunits and interaction with tropolone, Biochemistry 50 (2011) 5477–5486.
[16] F. García-Molina, J.L. Muñoz-Muñoz, M. Garcia-Molina, P.A. Garcia-Ruiz, J. Tudela, F. Garcia-Canovas, J.N. Rodriguez-Lopez, Melanogenesis inhibition due to NADH, Biosci. Biotechnol. Biochem. 74 (2010) 1777–1787.
[17] F. García-Molina, J.L. Muñoz-Muñoz, J.R. Acosta, P.A. Garcia-Ruiz, J. Tudela, F. Garcia-Canovas, J.N. Rodriguez-Lopez, Melanogenesis inhibition by tetrahydropterines, Biochim. Biophys. Acta 1794 (2009) 1766–1774.
[18] F. García-Molina, J.L. Muñoz-Muñoz, F. Martinez-Ortiz, P.A. Garcia-Ruiz, J. Tudela, F. Garcia-Canovas, J.N. Rodriguez-Lopez, Tetrahydrofolic acid is a potent suicide substrate of mushroom tyrosinase, J. Agric. Food Chem. 59 (2011) 1383–1391.
[19] F. Garcia-Molina, A.N. Hiner, L.G. Fenoll, J.N. Rodriguez-Lopez, P.A. Garcia-Ruiz, F. Garcia-Canovas, J. Tudela, Mushroom tyrosinase: catalase activity, inhibition and suicide inactivation, J. Agric. Food Chem. 53 (2005) 3702–3709.
[20] J.L. Munoz-Munoz, F. Garcia-Molina, P.A. Garcia-Ruiz, R. Varon, J. Tudela, J.N. Rodriguez-Lopez, F. Garcia-Canovas, Catalytic oxidation of aminophenols and aromatic amines by mushroom tyrosinase, Biochim. Biophys. Acta 1814 (2011) 1974–1983.
[21] J.N. Rodriguez-Lopez, L.G. Fenoll, P.A. Garcia-Ruiz, R. Varon, J. Tudela, R.N. Thorneley, F. Garcia-Canovas, Stopped-flow and steady-state study of the diphenolase activity of mushroom tyrosinase, Biochemistry 39 (2000) 10497–10506.
[22] L. Fenoll, M.J. Peñalver, J.N. Rodriguez-Lopez, P.A. Garcia-Ruiz, F. Garcia-Canovas, J. Tudela, Deuterium isotope effect on the oxidation of monophenols and *o*-diphenols by tyrosinase, Biochem. J. 380 (2004) 643–650.
[23] M.J. Penalver, J.N. Rodriguez-Lopez, P.A. Garcia-Ruiz, F. Garcia-Canovas, J. Tudela, Solvent deuterium isotope effect on the oxidation of *o*-diphenols by tyrosinase, Biochim. Biophys. Acta 1650 (2003) 128–135.
[24] O. Toussaint, K. Lerch, Catalytic oxidation of 2-aminophenols and ortho hydroxylation of aromatic amines by tyrosinase, Biochemistry 26 (1987) 8567–8571.
[25] B. Gasowska, P. Kafarski, H. Wojtasek, Interaction of mushroom tyrosinase with aromatic amines, *o*-diamines and *o*-aminophenols, Biochim. Biophys. Acta 1673 (2004) 170–177.
[26] F. Maddaluno, K.F. Faull, Inhibition of mushroom tyrosinase by 3-amino-L-tyrosine: molecular probing of the active site of the enzyme, Experientia 44 (1988) 885–887.
[27] A. Rescigno, E. Sanjust, A.C. Rinaldi, F. Sollai, N. Curreli, A. Rinaldi, Effect of 3-hydroxyanthranilic acid on mushroom tyrosinase activity, Biochim. Biophys. Acta 1384 (1998) 268–276.
[28] O.H. Lowry, N.J. Rosebrough, A.L. Farr, R.J. Randall, Protein measurement with the folin phenol reagent, J. Biol. Chem. 193 (1951) 265–275.
[29] J.N. Rodriguez-Lopez, M. Banon-Arnao, F. Martinez-Ortiz, J. Tudela, M. Acosta, R. Varon, F. Garcia-Canovas, Catalytic-oxidation of 2,4,5-trihydroxyphenylalanine by tyrosinase-identification and evolution of intermediates, Biochem. Biophys. Acta 1160 (1992) 221–228.
[30] F. Garcia-Molina, J.L. Muñoz, R. Varon, J.N. Rodriguez-Lopez, F. Garcia-Canovas, J. Tudela, A review on spectrophotometric methods for measuring the monophenolase and diphenolase activities of tyrosinase, J. Agric. Food Chem. 55 (2007) 9739–9749.
[31] J.L. Munoz, F. Garcia-Molina, R. Varon, J.N. Rodriguez-Lopez, F. Garcia-Canovas, J. Tudela, Calculating molar absorptivities for quinones: application to the measurement of tyrosinase activity, Anal. Biochem. 351 (2006) 128–138.
[32] J.N. Rodriguez-Lopez, J.R. Ros-Martinez, R. Varon, F. Garcia-Canovas, Calibration of a Clark-type oxygen electrode by tyrosinase-catalyzed oxidation of a 4-*tert*-butylcatechol, Anal. Biochem. 202 (1992) 356–360.
[33] Jandel Scientific, Sigma Plot 9.0 for Windows™, Jandel Scientific, Core Madera, 2006.
[34] J.L. Muñoz-Muñoz, J. Berna, F. Garcia-Molina, P.A. Garcia-Ruiz, J. Tudela, J.N. Rodriguez-Lopez, F. Garcia-Canovas, Unravelling the suicide inactivation of tyrosinase: a discrimination between mechanisms. J. Mol. Catal. B Enzym. (2011), Doi: 10.1016/j.molcatb.2011.11.001.
[35] S. Menon, R.W. Fleck, G. Yong, K.G. Strothkamp, Benzoic acid inhibition of the α, β, and γ isoenzymes of *Agaricus bisporus* tyrosinase, Arch. Biochem. Biophys. 280 (1990) 27–32.
[36] J.S. Conrad, S.R. Dawso, E.R. Hubbard, T.E. Meyers, K.G. Strothkamp, Inhibitor binding to the binuclear active site of tyrosinase: temperature, pH and solvent deuterium isotope effects, Biochemistry 33 (1994) 5739–5744.
[37] H. Decker, R. Dillinger, F. Tuczek, How does tyrosinase work? Recent insights from model chemistry and structural biology, Angew. Chem. Int. Ed. 39 (2000) 1591–1595.
[38] A. Rescigno, F. Bruyneel, A. Padiglia, F. sollai, A. Salis, J. Marchand-Brynaert, E. Sanjust, Structure-activity relationships of various amino-hydroxy-benzenesulphonic acids and sulphonamides as tyrosinase substrates, Biochim. Biophys. Acta 1810 (2011) 799–807.